"EFFECT OF SEISMIC WAVE PROPAGATION ON BURIED PIPELINES"

by Michael O'Rourke[I] and Gerardo Castro[II]

SUMMARY

The effect of seismic wave propagation on straight buried pipelines is investigated in this paper. Underlying assumptions for the presently available analysis procedure are studied using ground motions recorded at building sites during the 1971 San Fernando Earthquake. It is shown that the propagation velocity of seismic waves with respect to the ground surface is a critical parameter vis-a-vis the assumption that spatial variations in ground motions may be neglected. Propagation velocities of seismic waves with respect to the ground surface are presented for five Japanese Earthquakes as well as for the recent 1979 Imperial Valley Earthquake.

INTRODUCTION

Seismic wave propagation effects are one of three major causes of damage to buried pipeline during earthquakes. Surface faulting and major ground failure such as soil liquefaction and land sliding are the other two major causes of damage. Because of the finite propagation velocity of seismic waves along the ground surface, ground motion at two points along a propagation path of seismic waves will be out of phase. A buried pipeline aligned along the propagation path would then be subjected to strains and curvatures induced by these out-of-phase motions.

ANALYSIS PROCEDURE FOR WAVE PROPAGATION EFFECTS

Simplified relations for the analysis of buried pipelines for wave propagation effects have been developed by Newmark (1). Two assumptions underline these relationships. First, it is assumed that the motion of the pipeline is the same as the motion of the surrounding soil. There seems to be fairly wide agreement on this first assumption. The second assumption deals with the ground motion generated by the earthquake. It is assumed that the seismic excitation may be modeled as a traveling wave. That is, spatial variations in ground displacements may be neglected. Using the above assumptions, Newmark (1) has shown that the axial strain induced in the pipeline, ε, becomes

$$\varepsilon = V_{max}/C \qquad (1)$$

where V_{max} = maximum ground or particle velocity and C = propagation velocity of seismic waves with respect to the pipeline. A similar relationship for maximum curvature was also developed by Newmark but does not govern pipeline design for reasonable values of ground motion parameters.

I.,II. Associate Prof., and Graduate Student respectively, Dept. of Civil Engineering, Rensselaer Polytechnic Inst., Troy, New York 12181

EFFECT OF SPATIAL VARIATION IN GROUND MOTION TIME HISTORIES

The analysis procedure described above neglects any spatial variation of the ground displacement time histories. That is, ground displacement time histories at two points along the same epicentral line are assumed to be identical except for a time lag, τ, related to the separation distance and the propagation velocity of the seismic waves with respect to the ground surface. Differences in the propagation velocities of various types of seismic waves as well as possible variations in the material properties along the propagation path would both tend to cause spatial variations in ground displacements. The effect of the spatial variations in ground motion vis-a-vis axial pipeline strain was investigated using ground motions recorded during the 1971 San Fernando Earthquake. A total of 22 pairs of ground displacement time histories were used in the investigation. Each pair of ground displacements are for two nearby stations lying roughly along radial lines from the epicenter. The 22 pairs of recordings were derived from double intergration of corrected accelerograms. Listed in Table 1 are the names, identification numbers and approximate separation distance between the pairs of stations used in this comparison. Although most of the displacement time histories were for the basements of structures, it is assumed, herein, that they represent free field conditions. While it is recognized that this assumption is important, the authors are unable at the present time to gauge the effect of this assumption.

The four horizontal ground displacement components for each pair of stations were used to generate two radial ground displacement time histories using standard coordinate transformation techniques. Recording stations triggered independently during the San Fernando Earthquake. To eliminate the effect of this independent triggering, a cross correlation function was used to match the radial components at the two stations.

Two strains were calculated for each pair of stations assuming various values for the time lag, τ, that is, the time required for the seismic excitation to propagate from one station to the other. The first strain $\varepsilon_1(\tau)$ corresponds to the maximum value of the average strain between two stations using the actual radial displacement time histories

$$\varepsilon_1(\tau) = \left|X(t) - \hat{Y}(t - \tau)\right|_{max}/L \qquad (2)$$

where $X(t)$ is the radial component at the first station and $\hat{Y}(t)$ is the radial component of the station furthest from the epicenter modified for the effect of independent triggering of the recorded instruments, and L is the separation distance between the pair of stations. The second strain $\varepsilon_2(\tau)$ is that predicted by Eq. 1

$$\varepsilon_2(\tau) = V_{max} \cdot \tau/L \qquad (3)$$

The two strains $\varepsilon_1(\tau)$ and $\varepsilon_2(\tau)$ were computed for various values of the time lag τ for all 22 pairs of recordings. Fig. 1 is a normalized representative plot of the two strains. Fig. 1 can be used to gauge the effect of spatial variation in ground motion upon pipeline strain. If the actual time lag is such that $\varepsilon_2 > \varepsilon_1$ then spatial variation in ground motion can be neglected. If, on the other hand, $\varepsilon_2 < \varepsilon_1$ then spatial variations can not be neglected.

The time lag for which the two strains are equal is defined as the cross-over time lag, τ_c

$$\varepsilon_1(\tau_c) = \varepsilon_2(\tau_c) \tag{4}$$

Referring to Fig. 1, if the actual time lag is less than τ_c than spatial variations in ground motion can not be neglected. The cross-over time lag for each of the 22 pairs of stations are also listed in Table 1. Note that τ_c is relatively independent of separation distance and ranges from about 0.2 seconds to 1.2 seconds. The average value of the cross-over time lag is about 0.6 seconds. The final item listed In Table 1 is the separation distance L divided by the cross-over time lag τ_c. The ratio L/τ_c is the propagation velocity for which the actual time lag equals the cross-over time lag. If the actual propagation velocity is greater than L/τ_c then the spatial variations in ground motion can not be neglected.

PROPAGATION VELOCITIES WITH RESPECT TO GROUND SURFACE

Japanese researchers have established arrays of seismometers which yield information about the propagation velocity of seismic waves with respect to the ground surface. Tsuchida and Kurata (4) established a horizontal array consisting of six sets of seismometers located at 500 meter intervals along a 2500 meter line. Using cross correlation techniques, Tsuchida and Kurata were able to establish the propagation velocities for three earthquakes which occured during the summer of 1974. Table 2 presents the date, magnitude, focal depth and epicentral distance for the three earthquakes as well as calculated propagation velocities with respect to the ground surface due to these earthquakes. Similar information developed by Tamura et.al., (3) also appear in Table 2.

A preliminary report (2) on the recent 1979 Imperial Valley Earthquake contains information which can be used to calculate similar information for West Coast U.S. Earthquakes. Epicentral distances, WWVB triggering time and the interval between triggering and the arrival of the first shear wave (S!) is available for 18 stations. Plotting distance traveled versus absolute time yields a value of 3.7 km/sec. as the propagation velocity with respect to the ground surface of S!. Although the method used above for Imperial Valley is different than that used by the Japanese, the value of 3.7 km/sec. falls in the range of values for Japan.

CONCLUSIONS

Since the propagation velocities in Table 2 are all considerably larger than the cross-over velocity, L/τ_c, in Table 1, it appears that spatial variations in ground motions can not be neglected when determining axial strain induced in pipelines by earthquakes. This conclusion must be tempered, however, by the fact that motions recorded at buildings were used in this investigation as opposed to true free field motions.

ACKNOWLEDGEMENTS

Support of this work by the National Science Foundation through Grant No. ENV76-14884 and PFR78-15856 is gratefully acknowledged.

REFERENCES

1. Newmark, N., (1967) "Problems in Wave Propagation in Soil and Rock", Proc. Inter. Symp. on Wave Propagation and Dynamic Properties of Earth Materials, Albuquerque, p. 7-26.
2. Porcella, R. and Matthiesen, R., (1979) Strong Motion Records, Oct. 15, 1979 Imperial Valley Earthquake, U.S.G.S. Open-File Rpt. 79-1654, 42p.
3. Tamura, C., Noguchi, T. and Kato, K., (1977) "Earthquake Observations Along Measuring Lines on the Surface of Alluvial Soft Ground", Proc. Sixth World Conf. on Earthquake Eng., New Delhi, pp. 2-63 to 2-68.
4. Tsuchida, H. and Kurata, E., (1976) "Observed Earthquake Ground Displacements Along a 2500 Meter Line", Proc. U.S.-Japan Seminar on Earthquake Engineering Research with Emphasis on Lifeline Systems, pp. 29-42.

STATION 1 Name	I.D.#	STATION 2 Name	I.D.#	L (m)	cross-over time lag τ_c(sec)	L/τ_c (m/sec)
616 S. Normandie	J148	3411 Wilshire	S265	220	0.30	733
616 S. Normandie	J148	3550 Wilshire	S266	150	0.25	600
1800 Cen.Park E.	I134	1880 Cen.Park E.	N188	50	0.31	161
611 W. Sixth	G112	646 S. Olive	F098	190	1.20	158
420 S. Grand	K157	646 S. Olive	F098	370	0.50	740
1880 Cen.Park E.	N188	1900 Ave.Stars	R249	190	0.45	422
1800 Cen.Park E.	I134	1900 Ave.Stars	R249	230	0.20	1150
445 Figueroa	C054	611 W. Sixth	G112	350	0.40	875
533 S. Fremont	R253	646 S. Olive	F098	580	0.78	743
445 Figueroa	C054	646 S. Olive	F098	580	1.20	483
646 S. Olive	F098	808 S. Olive	F089	210	0.80	262
611 W. Sixth	G112	808 S. Olive	F089	410	1.25	328
533 S. Fremont	R253	808 S. Olive	F089	760	0.60	1270
445 Figueroa	C054	808 S. Olive	F089	750	0.96	781
1900 Ave.Stars	R249	1901 Ave.Stars	D059	50	0.49	102
1760 N. Orchid	Q236	7080 Holly.Blvd.	D068	120	0.68	176
1760 N. Orchid	Q236	Hollywood Stor.	D057	1000	0.81	1230
616 S. Normandie	J148	3470 Wilshire	E075	210	0.70	300
535 S. Fremont	R253	611 W. Sixth	G112	390	0.72	541
6464 Sunset Blvd.	R246	Hollywood Stor.	D057	570	0.49	1160
1760 N. Orchid	Q236	6464 Sunset Blvd	R246	430	0.42	1024
1760 N. Orchid	Q236	6430 Sunset Blvd	R248	430	0.44	977

TABLE 1. Pairs of 1971 San Fernando Earthquake Stations

Date	Country	Mag.	Focal Depth (km)	Epic. Dis. (km)	Prop. Vel. (km/sec)
5/9/74	Japan	6.9	10	140	5.3
7/8/74	Japan	6.3	40	161	2.6
8/4/74	Japan	5.8	50	54	4.4
1/23/68	Japan	-	80	30	2.9
7/1/68	Japan	6.1	50	52	2.6
10/15/79	U.S.	6.4	Shallow	6-108	3.7

TABLE 2. Seismic Propagation Velocity With Respect to Horizontal Surface

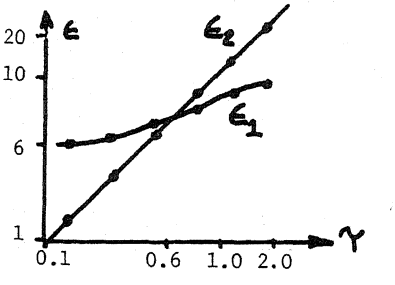

Fig. 1. Normalized strain vs τ